Journal of Molecular Catalysis A: Chemical 320 (2010) 85–91

Contents lists available at ScienceDirect

Journal of Molecular Catalysis A: Chemical

journal homepage: www.elsevier.com/locate/molcata

Synthesis and characterization of γ-Bi_2MoO_6 prepared by co-precipitation: Photoassisted degradation of organic dyes under vis-irradiation

A. Martínez-de la Cruz*, S. Obregón Alfaro

Facultad de Ingeniería Mecánica y Eléctrica, Universidad Autónoma de Nuevo León, Pedro de Alba s/n, Ciudad Universitaria, C.P. 66451, San Nicolás de los Garza, N.L., Mexico

ARTICLE INFO

Article history:
Received 12 November 2009
Received in revised form 14 January 2010
Accepted 17 January 2010
Available online 25 January 2010

Keywords:
γ-Bi_2MoO_6
Molybdates
Photocatalysis
Photosensitization

ABSTRACT

γ-Bi_2MoO_6 was prepared by the co-precipitation method at 450 °C. The molybdate was characterized by X-ray diffraction (XRD), scanning and transmission electron microscopy (SEM and TEM), simultaneous thermogravimetric and differential thermal analysis (TGA/DTA), diffuse reflectance spectroscopy (DRS), and surface analysis (BET). The synthesized material was tested as photocatalyst for the degradation of rhodamine B (rhB), indigo carmine (IC), and methyl orange (MO) under visible light irradiation. The γ-Bi_2MoO_6 photocatalyst showed the capacity to bleach the dye solution in the following sequence: indigo carmine (IC) > rhodamine B (rhB) > methyl orange (MO). The degradation of rhB by γ-Bi_2MoO_6 seems to happen predominantly through the photosensitization of the organic dye by the action of visible light irradiation. On the other hand, the IC degradation simultaneously happens by photosensitization and true photocatalytic processes. The activity of γ-Bi_2MoO_6 for the degradation of MO was negligible. The reached mineralization degrees after 100 h of irradiation were 86% for rhB and 80% for IC.

1. Introduction

Heterogeneous photocatalysis represents an important scientific field due to its potential technological applications to solve environmental issues related to water purification and alternative energy applications [1,2]. The semiconductor/energy-radiation combination produces the ejection of an electron (e^-) from the valence band to the conduction band in the semiconductor, and the concomitant generation of a hole (h^+) in the valence band. The successful migration of both charges to the surface of the semiconductor produces active sites where organic pollutants can be oxidized or reduced.

In the search of semiconductor materials with photocatalytic activity under visible light irradiation, several efforts have been carried out in the last decade. For example, the TiO_2 anatase polymorph has been doped with nitrogen in order to increase its absorption in the visible range [3]. In other direction, several authors have proposed alternative oxides to traditional TiO_2 with high photocatalytic activity under visible light irradiation such as $In_{1-x}Ni_xTaO_4$ [4], $CaIn_2O_4$ [5], $InVO_4$ [6], and $BiVO_4$ [7].

Recently, Shimodaira et al. reported the ability of molybdates belonging to the Bi_2O_3–MoO_3 system to act as photocatalysts in the O_2 evolution from an $AgNO_3$ solution by using visible light irradiation [8]. Their work has opened a new field of application of the molybdates as photocatalysts on heterogeneous photocatalytic reactions. In the last three years, several authors have reported the efficiency of the γ-Bi_2MoO_6 oxide as photocatalyst for the degradation of organic pollutants under visible light irradiation, see Table 1. The number of published papers in the last years reveals an increasing interest in the search of possible applications of γ-Bi_2MoO_6 as photocatalyst in the visible region. In this sense, different synthesis routes have been proposed in order to get a material with better textural properties and, consequently, higher photocatalytic activity.

So far, the most common preparation method used to synthesize bismuth molybdates is by the co-precipitation from bismuth nitrate and ammonium molybdate in aqueous media. This route provides an easy and inexpensive way to prepare molybdates at lower temperatures than those employed in the solid-state reaction. The method implies the co-precipitation of the pure hydroxides and the precipitation of bismuth with polymerized molybdenum ions. These inorganic intermediates can be easily decomposed by using temperatures of synthesis of 300–400 °C below those used in the solid-state reaction. Surprisingly enough, the photocatalytic activity of the γ-Bi_2MoO_6 oxide synthesized by the co-precipitation method has been not reported.

In this work, the photocatalytic activity of the γ-Bi_2MoO_6 oxide synthesized by the co-precipitation method is explored. For this purpose, three organic dyes of different families such as rhodamine B (rhB, xanthane, C.I. number 45170), indigo carmine (IC, indigoid, C.I. number 73015), and methyl orange (MO, azo, C.I. number 13025) were selected, see Fig. 1. The previous works about the

* Corresponding author. Tel.: +52 81 83 29 40 20.
E-mail address: azael70@yahoo.com.mx (A. Martínez-de la Cruz).

1381-1169/$ – see front matter © 2010 Elsevier B.V. All rights reserved.
doi:10.1016/j.molcata.2010.01.008

Table 1
Previous works on the photocatalytic activity of γ-Bi_2MoO_6 prepared by different synthesis routes.

Preparation	Morphology	Band gap, E_g (eV)	Photocatalytic reaction	Reference
Solid-state reaction/reflux	–	2.70	O_2/$AgNO_3$	[8]
Hydrothermal	Nanoplates, 15–30 nm	2.70–2.80	O_2/$AgNO_3$	[9]
	Nanoplates, 200–400 nm	2.88	rhB	[10]
	Nanosheets, 500 nm	2.56–2.59	rhB	[11]
	Nanoplates, 200 nm	2.59	rhB and MB	[12]
Amorphous complex precursor	Nanoparticles, 30–200 nm	2.33–2.59	rhB	[13]
Hydrothermal/microwave	Nanoplates, 100–200 nm	–	MB	[14]
Dip coating	Thickness film 100 nm	2.67	K-2G, Red X-3B, KD-3G	[15]
	Thickness film 69 nm	2.61	Photoresponse	[16]
			ibuprofen and naproxen	[17]
Solvothermal/microwave	Nanorods, Ø 30 nm; Nanosheets and nanobelts	2.53	rhB	[18]
Ultrasound/calcination	Nanoparticles, 150 nm	2.63	rhB	[19]
Molten salt	Flake-like nanoparticles, 50–200 nm	2.60	rhB	[20]
Citrate method	–	2.58	rhB	[21]

rhB, rhodamine B and MB, methylene blue.

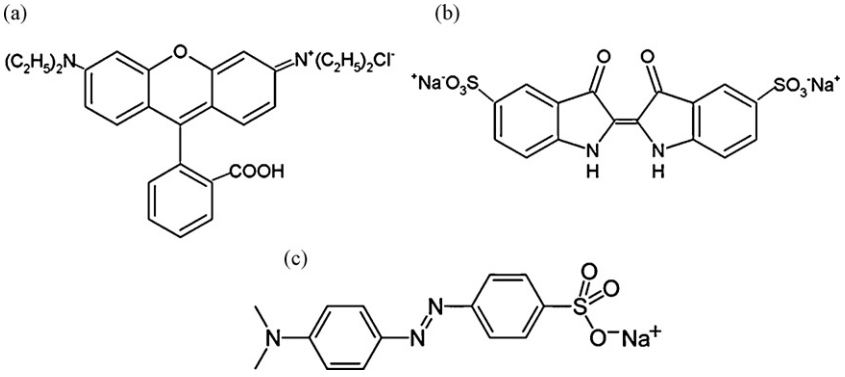

Fig. 1. Molecular structure of (a) rhodamine B, (b) indigo carmine, and (c) methyl orange.

photocatalytic activity of the γ-Bi_2MoO_6 oxide have been mainly limited to the degradation of rhB as it is shown in Table 1. By taking into account the importance of the functional groups of an organic dye in the rate of a photocatalytic reaction, the analysis of the photoactivity of the γ-Bi_2MoO_6 oxide for the degradation of different types of organic compounds could determine its future application in the field of wastewater treatment. Finally, some aspects of the reaction mechanism will be discussed in order to contribute to the state of knowledge of the degradation of organic dyes by the γ-Bi_2MoO_6 oxide.

2. Experimental

2.1. Preparation of γ-Bi_2MoO_6 samples

The γ-Bi_2MoO_6 oxide was synthesized by the so-called co-precipitation method. The method implies the preparation of two aqueous solutions. In the first one, 9.5439 g of $Bi(NO_3)_3{\cdot}5H_2O$ [Aldrich, 99.99%] was dissolved in 100 mL of HNO_3 (10%, v/v). The second one was prepared by dissolving 1.7369 g of $(NH_4)_6Mo_7O_{24}{\cdot}4H_2O$ [Productos Químicos Monterrey, 99%+] in 100 mL of distilled water. The bismuth nitrate solution was added dropwise (~5 mL min^{-1}) to the molybdate solution. This process was accompanied with vigorous stirring. When the mix was reached, the pH of the solution was adjusted at 3 by using NH_4OH. The resulting yellow suspension was maintained at 70 °C to promote the slow evaporation of the solvent. The yellow powder obtained after this thermal treatment was used as precursor of γ-Bi_2MoO_6. A slow thermal treatment of 5 °C min^{-1} in air at 400 and 450 °C for 20 h was employed to obtain polycrystalline powders of γ-Bi_2MoO_6. The thermal treatments were carried out until the mass loss of the material was negligible. For comparative purposes, a sample of γ-Bi_2MoO_6 was also synthesized by solid-state reaction between Bi_2O_3 [Aldrich, 99.9%+] and MoO_3 [Merck, 99.9%+]. A stoichiometric mixture was placed in a porcelain crucible and then heated at 550 °C for 96 h to obtain the binary oxide.

2.2. Sample characterization

The structural characterization was carried out by X-ray powder diffraction using a Bruker D8 Advanced diffractometer with CuK_α radiation, equipped with a Vantec high speed detector. The X-ray diffraction data of the samples were collected in the 2θ range of 10–70° with a scan rate step of 0.05° 0.05 s^{-1}. The morphology of the samples was analyzed by scanning electron microscopy (SEM), using a JSM JEOL 6490 LV microscope with an accelerating voltage of 30 kV. The particle size of the samples was observed by transmission electron microscopy (TEM). For this purpose, a JEOL 2010 instrument with an accelerating voltage of 200 kV was used.

Thermogravimetric and differential thermal analyses (TGA/DTA) of the precursor were performed on a TA Instruments Mod SDT Q600 thermal analyzer. The measurements were

carried out under nitrogen atmosphere with a flux of 100 mL min^{-1} and a heating rate of 5 °C min^{-1}. The surface area (BET) of the photocatalysts was determined by N_2 adsorption–desorption measurements by using a Bel-Japan Minisorp II Surface Area & Pore Size analyzer. The adsorption–desorption isotherms were evaluated at −196 °C after a pretreatment of the sample at 100 °C for 4 h. UV-diffuse reflectance spectra of the photocatalysts were measured by using a UV–vis spectrophotometer equipped with an integration sphere (Perkin Elmer Lambda 35).

2.3. Photocatalytic reactions

The photochemical reactor employed in this work consisted in a borosilicate glass beaker surrounded with a water jacket to maintain the reaction temperature at 25 ± 1 °C. A Xe lamp of 10,000 K with a luminous flux of 2100 lm was used as irradiation source. The emission spectrum of the Xe lamp was measured on a UV–vis spectrophotometer. A negligible contribution of UV radiation was observed ($\lambda < 390$ nm); moreover, this one was filtered by the borosilicate container. Additionally, some experiments with UV-irradiation of 365 nm were also performed (1250 μW cm^{-2}). The photocatalytic activity of γ-Bi_2MoO_6 was evaluated for the degradation reaction of three organic dyes (rhB, IC, and MO) in aqueous solution. Considering the molar extinction coefficient of each dye, the initial concentrations were 5 mg L^{-1} for rhB, 30 mg L^{-1} for IC, and 20 mg L^{-1} for MO. In a glass beaker, 220 mL of the dye solution containing 220 mg of photocatalyst were placed in an ultrasonic bath for 10 min to eliminate aggregates. In order to achieve the adsorption–desorption equilibrium of the dye on the catalyst surface, the solution was left in the dark for 1 h. After this period of time, the light source was turned on. Samples with different light-irradiation times were taken and analyzed as described in a previous work [22]. During the reaction, 6-mL aliquots were taken from the reactor at different time intervals followed by the separation of the photocatalyst through double centrifugation (4000 rpm, 20 min). The supernatant solution was decanted and the dye concentration was determined through its absorption band maximum by using a UV–vis spectrophotometer (Perkin Elmer Lambda 35).

The mineralization degree of the rhB and IC was monitored by the total organic carbon (TOC) analysis of the solutions with different irradiation times. The TOC analysis was performed by adding an acidified potassium persulfate reagent to the samples for their oxidation, followed by a digestion process at 105 °C for 2 h. The evolved CO_2 was analyzed by a colorimetric method in an HACH DR/890 colorimeter according to the procedure supplied by the HACH Company [23]. In a typical experiment, 220 mL of the corresponding dye solution (20 mg L^{-1} for rhB and 30 mg L^{-1} for IC) containing 660 mg of photocatalyst were employed.

Some photocatalytic experiments were carried out in the presence of 2-propanol in order to determine some aspects of the dye degradation mechanism. The followed procedure was similar to the one cited above, but in this case, 2-propanol was added until getting a final concentration of 1×10^{-4} mol L^{-1} in the dye solution employed in the photocatalytic experiments.

3. Results and discussions

3.1. Sample characterization

Pale-yellow powder was obtained as product of the co-precipitation process of the bismuth and molybdenum ions. This material will be identified hereafter as precursor. The decomposition of the precursor to form γ-Bi_2MoO_6 was followed by TGA/DTA

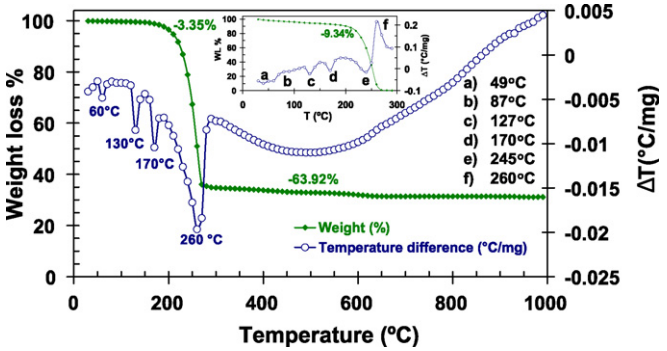

Fig. 2. TGA and DTA analyses of the precursor used to prepare the γ-Bi_2MoO_6 photocatalyst. In the insert, the TGA/DTA analysis of the thermal decomposition of NH_4NO_3 is shown.

simultaneous analysis, as it is shown in Fig. 2. An initial weight loss of 3.35% was observed at temperatures below 200 °C, which corresponds to the water evaporation of adsorbed and occluded water on the precursor. The main thermal event took place between 200 and 270 °C and corresponds to the elimination of gases as products of the decomposition of nitrates and ammonium salts. After 270 °C, there was no evidence of weight losses. Three endothermic peaks without weight losses were observed near 60, 130, and 170 °C. A fourth endothermic peak associated with the main precursor weight loss was observed at 260 °C. Previously, Reilly et al. [24] reported similar endothermic peaks during the formation of γ-Bi_2MoO_6 when it was synthesized by co-precipitation starting from the same salts. The authors attributed the origin of the peaks to a rearrangement of the H bonds in the system. Nevertheless, a simpler explanation can be proposed from the analysis of the precursor formation. The use of an acidified solution of $Bi(NO_3)_3{\cdot}5H_2O$ with HNO_3 and the posterior neutralization with NH_4OH during the co-precipitation process lead to think that the formation of NH_4NO_3 as sub-product is feasible. To elucidate this point, a TGA/DTA analysis of NH_4NO_3 was carried out, see insert in Fig. 2. Three endothermic peaks associated with allotropic phase transitions of NH_4NO_3 were observed at 49, 87, and 127 °C. The melting point of the salt produced the fourth endothermic peak at 170 °C [25]. Finally, two successive peaks were observed at 245 °C (endothermic) and 260 °C (exothermic). The first thermal event can be associated with the boiling point of the salt; meanwhile the second one is due to the energy liberation of the system during the elimination of the N_2O and H_2O gases [26]. On the basis of these results, it is possible to conclude that the endothermic peaks observed during the decomposition of the γ-Bi_2MoO_6 precursor are associated with thermal events of the NH_4NO_3 sub-product. In the same way, the released energy during the decomposition of ammonium salt should be lower than the energy absorbed during the formation of γ-Bi_2MoO_6 (260 °C); and consequently, an endothermic peak was observed at this temperature.

The formation of the γ-Bi_2MoO_6 oxide was followed by the X-ray diffraction technique as it is shown in Fig. 3. In the first instance, the X-ray diffraction pattern of the precursor material shows the diffraction lines of NH_4NO_3 (JCPDS Card No. 47-0867), which is in concordance with the TGA/DTA results. When the precursor was calcined at 400 °C for 20 h, the γ-Bi_2MoO_6 crystal framework was formed (JCPDS Card No. 84-0787), but with a small impurity that was identified as Bi_2O_3 (JCPDS Card No. 65-1209). In order to eliminate the Bi_2O_3 without reacting, the precursor was heated at 450 °C for 20 h. As product of this thermal treatment, the γ-Bi_2MoO_6 oxide was obtained without impurities. This material was thoroughly characterized and then used as photocatalyst in photocatalytic experiments.

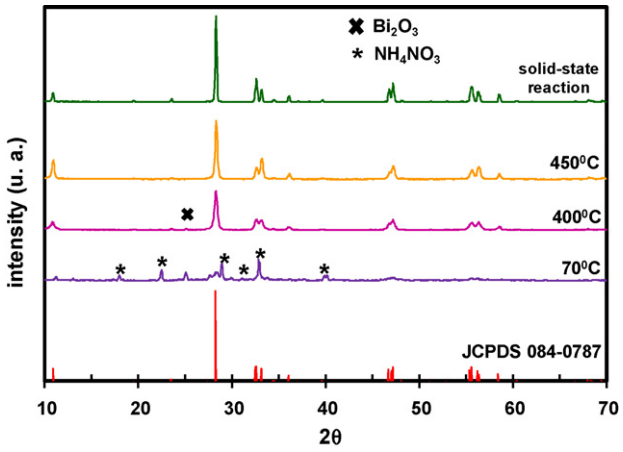

Fig. 3. XRD patterns of the powders obtained under different precursor calcination temperatures: (a) 70 °C, (b) 400 °C, (c) 450 °C, and a sample prepared by solid-state reaction (d) 550 °C.

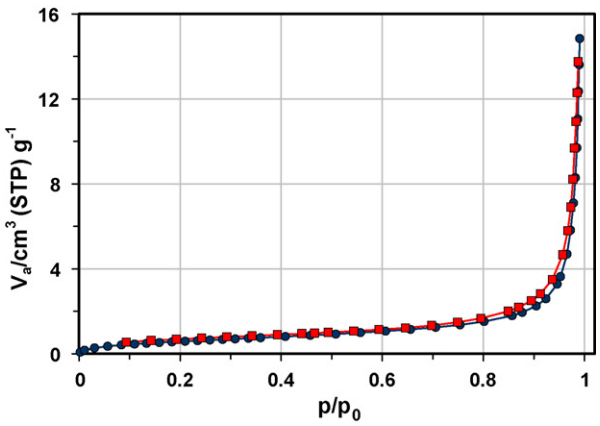

Fig. 5. N_2 adsorption–desorption isotherms for the sample prepared by the co-precipitation method at 450 °C.

The morphology of the γ-Bi_2MoO_6 oxide was studied by TEM and SEM analysis. Fig. 4a shows a TEM micrograph of the material obtained at 450 °C. A typical characteristic of the sample was its natural tendency to form aggregates, as corresponds to a material obtained by the co-precipitation method, where the formation and growth of the particles is uncontrolled [27]. In general, the sample showed an important heterogeneity in the shape of their particles whose sizes were higher than 200 nm. In Fig. 4b and c, the SEM micrographs show a material characterized by the agglomeration of the primary particles observed by TEM. These agglomerates reached values higher than 2 μm. The morphology of the sample obtained by solid-state reaction was very different. In the SEM micrograph in Fig. 4d, the formation of semi-ovoid particles with a regular distribution and sizes around of 1 μm can be observed.

The BET surface area was measured for the synthesized γ-Bi_2MoO_6 oxide. Fig. 5 shows the N_2 adsorption–desorption isotherms for the samples prepared at 450 °C. According to the classification developed by deBoer [28], the isotherm profile can be associated with type II. This type of isotherm is characteristic of a material that is not porous or possibly macroporous with high adsorption energy. The surface area obtained for the sample calcined at 450 °C (2.3 $m^2\,g^{-1}$) is in good agreement with some published data using the co-precipitation method at similar temperatures [29]. This surface area is 4 times higher than the value observed for the sample prepared by solid-state reaction at 550 °C, which was 0.6 $m^2\,g^{-1}$.

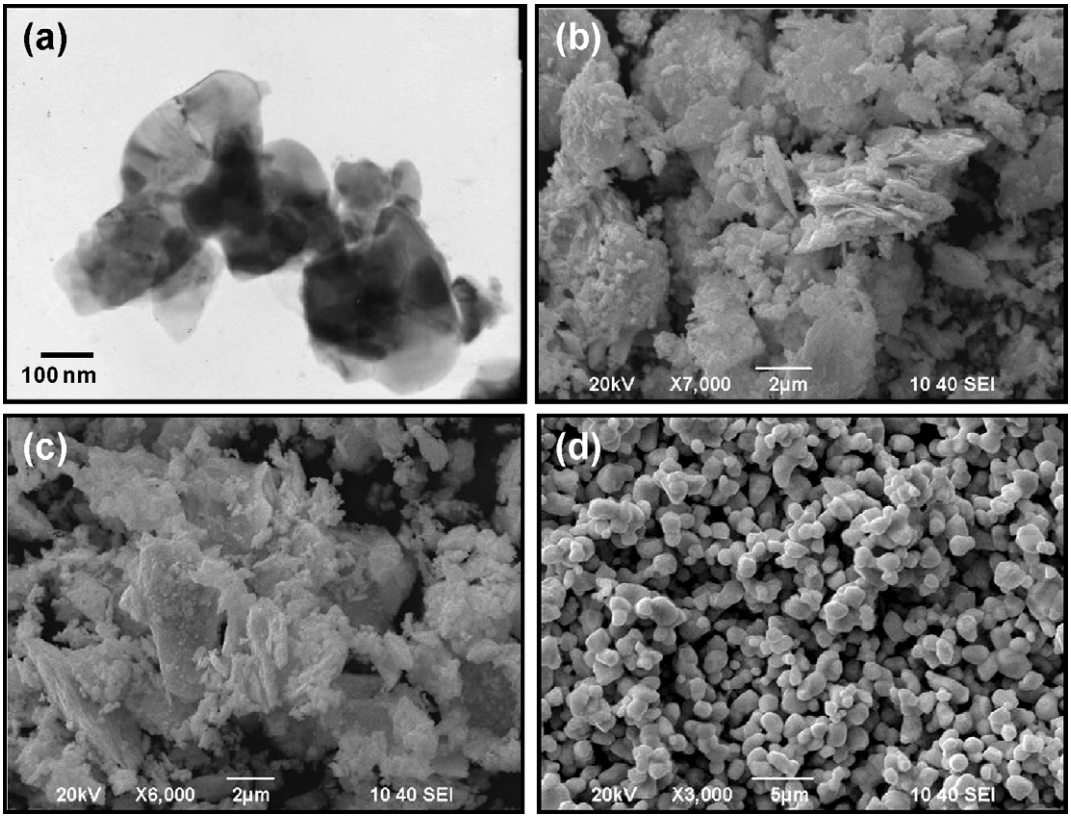

Fig. 4. TEM analysis of the morphology of γ-Bi_2MoO_6 synthesized at 450 °C by the co-precipitation method (a), SEM analysis of the same sample (b and c), and of a sample prepared by solid-state reaction (d).

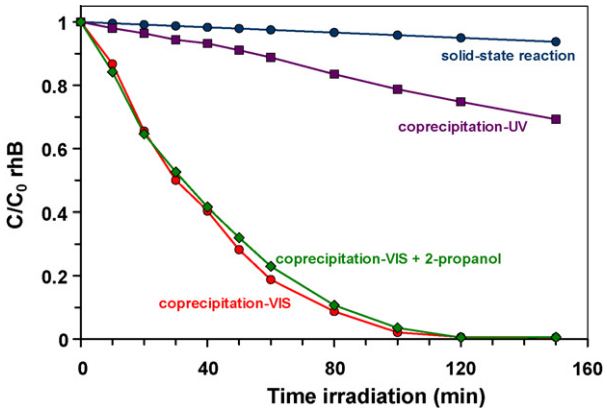

Fig. 6. Changes in the rhB concentration during its photocatalytic degradation (5 mg L^{-1}) in the presence of γ-Bi_2MoO_6.

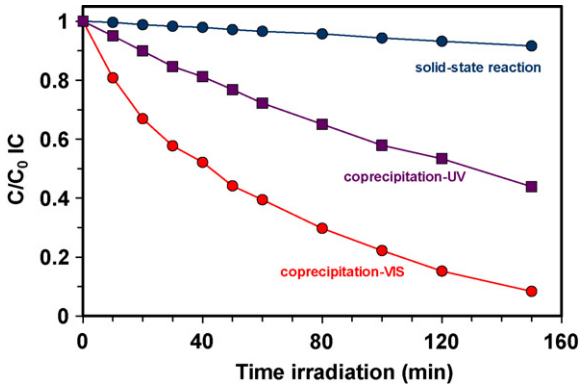

Fig. 7. Changes in the IC concentration during its photocatalytic degradation (30 mg L^{-1}) in the presence of γ-Bi_2MoO_6.

Diffuse reflectance spectra of the samples obtained at 450 °C by co-precipitation, and at 550 °C by solid-state reaction were measured by UV–vis spectroscopy. A shift to the blue of the absorption edges spectra was observed for the sample obtained by co-precipitation method. This phenomenon can be associated with the presence of an amount of amorphous material on the synthesized samples [30]. The band gaps (E_g) obtained for the samples were 2.44 eV (co-precipitation method) and 2.51 eV (solid-state reaction). These values are similar to those previously reported, see Table 1.

3.2. γ-Bi_2MoO_6 photocatalytic activity

The first studied case was the degradation of rhB, which is a dye characterized by the presence of a xanthene nucleus, see Fig. 1a. The temporal evolution of the dye concentration during the photodegradation process by γ-Bi_2MoO_6 is shown in Fig. 6. In the first instance, the sample obtained by the co-precipitation method showed a considerably higher photocatalytic activity than the one observed when the sample obtained by solid-state reaction was used as photocatalyst under visible light irradiation. The kinetic data can be adjusted according with a first-order reaction equation following the Langmuir–Hinshelwood model. On the basis of this model, the half-life time for bleaching the color of rhB was $t_{1/2}$ = 29 min. This value is almost 50 times smaller that the one obtained for the sample prepared by solid-state reaction, $t_{1/2}$ = 1386 min. In fact, after 100 min of irradiation, the sample prepared by co-precipitation bleached the dye solution. The differences observed in the photocatalytic activity for both samples can be explained, in part, on the basis of their surface areas. The BET area analysis revealed that the co-precipitation sample exhibited a surface area value only 4 times higher than the one observed for the solid-state reaction sample. As it is well known, so many factors can affect the photocatalytic reaction rate. Beyond any doubt, the synthesis method plays an important role in the morphology and textural properties of the products. In this sense, the analysis by the SEM technique revealed important differences between the samples obtained by the two synthesis methods. Whereas the solid-state reaction provided a well syntherized material, the material obtained by the co-precipitation method was characterized by an irregular surface with probably more active sites for the oxidation of the dye.

The degradation of rhB by a photocatalyst can be done by two ways. Firstly, by a true photocatalytic process, where the irradiation over the photocatalyst promotes an electron from its valence band to the conduction band, and then the electron–hole pair is formed. The second possibility is through a photosensitization process, where the irradiation excites an electron from the dye and then, it is injected to the conduction band of the semiconductor oxide. In both processes, a series of consecutive reactions leads to the eventual mineralization of rhB to CO_2 and H_2O [31]. The degradation mechanism of rhB has not been elucidated when γ-Bi_2MoO_6 is used as photocatalyst. For this reason, an experiment similar to the one mentioned above was performed, but now the photocatalyst/dye dispersion was irradiated with UV light (365 nm). As it can be seen in Fig. 6, the photocatalytic activity of γ-Bi_2MoO_6 decreased considerably and after 100 min of UV-irradiation only 20% of the dye solution was bleached. This experiment revealed that the degradation of rhB by γ-Bi_2MoO_6 seems to happen predominantly through the photosensitization of the organic dye by the action of visible light irradiation. An additional experiment was carried out, but in this case, the semiconductor/dye solution was irradiated with visible light irradiation in the presence of 2-propanol. As it is well known, this alcohol is recognized as an efficient hydroxyl radical scavenger. In a mechanism, where the presence of the hydroxyl radical is determining (true photocatalysis), the addition of 2-propanol to the semiconductor/dye solution must have a negative effect on the photodegradation process. In fact, when an experiment was performed using TiO_2 as semiconductor photocatalyst in the presence of 2-propanol, the photocatalytic activity decreased in 40%. Nevertheless, this situation was different for the γ-Bi_2MoO_6 photocatalyst. Fig. 6 shows that the presence of 2-propanol has not an appreciable effect on the photocatalytic degradation of rhB. This result is in good agreement with the proposed mechanism, indicating that the photosensitization process rules the degradation of rhB when the γ-Bi_2MoO_6 oxide is used as photocatalyst.

Nowadays, the study of the photocatalytic activity of γ-Bi_2MoO_6 has been focused on the rhB dye. In a minor proportion, the study of the photocatalytic activity of γ-Bi_2MoO_6 for the degradation of other organic dyes such as MB has been reported, see Table 1. In this work, we have considered the importance of extending the study of the capacity of the γ-Bi_2MoO_6 photocatalyst for the degradation of other families of organic dyes. With this purpose, the photocatalytic activity of γ-Bi_2MoO_6 was also evaluated in the degradation of indigo carmine (IC), an organic dye of the indigoid type as it is shown in Fig. 1b. The temporal evolution of the IC concentration during the photodegradation process by γ-Bi_2MoO_6 is shown in Fig. 7. The profile of the concentration–time curve revealed a high photocatalytic activity of γ-Bi_2MoO_6 in the bleaching of a solution of IC with Co = 30 mg L^{-1} under visible light irradiation. After 100 min, about 78% of the dye solution was bleached, and this value reached 90% after 150 min. Note that the initial IC concentration used in these experiments was 6 times higher than the one employed for rhB due to their respective molar extinction coefficients. Although the photocatalytic activity decreased when

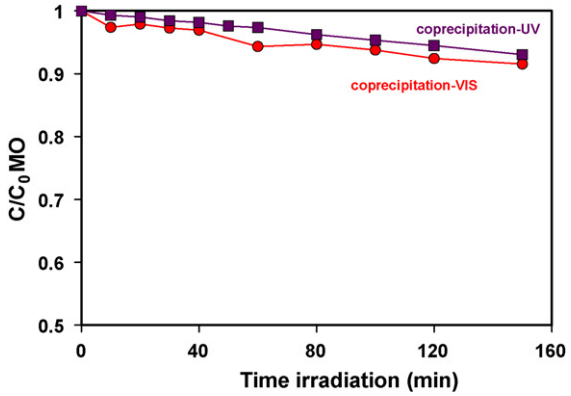

Fig. 8. Changes in the MO concentration during its photocatalytic degradation (20 mg L^{-1}) in the presence of γ-Bi_2MoO_6.

the dispersion was irradiated with UV-irradiation (365 nm), a considerable activity was observed in this experiment. This situation suggests that the two possible mechanisms of dye degradation take place simultaneously, i.e. true photocatalysis and photosensitization process. Finally, as it was expected, the IC degradation for the sample prepared by solid-state reaction was negligible.

The third dye tested in this work belonging to a family of dyes extensively employed in the industry and characterized by the presence of one or more azo groups. Within this family of compounds, methyl orange was selected (MO), see Fig. 1c. The high recalcitrant behavior of MO to its elimination from aqueous solutions under visible- and UV-irradiation is shown in Fig. 8. The recalcitrant behavior observed for MO can be explained on the basis of the presence of an azo group in its organic molecule, see Fig. 1c. As has been reported previously [32], the degradation of an azo-dye solution is associated with the broken of the bond –N=N–. Nevertheless this process is complicated because the average bond energy of the bond –N=N– is near to 420 kJ mol^{-1}. In the rhB case, for example, the degradation of the dye solution takes place for a successive de-ethylation (–N–C– = 286 kJ mol^{-1}). As a first conclusion, it is possible to establish that the γ-Bi_2MoO_6 photocatalyst showed the capacity to bleach the dye solution in the following sequence: indigo carmine (IC) > rhodamine B (rhB) > methyl orange (MO).

To determine the mineralization degree of the analyzed dyes by γ-Bi_2MoO_6, TOC analyses were performed on dispersions with different irradiation times. These data showed that the mineralization of rhB and IC by the γ-Bi_2MoO_6 photocatalyst is feasible, see Fig. 9. This is an important point due to the fact that the complete de-ethylation of rhB leads to the solution bleaching, but not necessarily to the mineralization of the dye. The TOC experiments elucidate this point. The bleaching of the dye solution is beyond the inactivation of the chromophore groups in the molecular structure. The mineralization degrees reached after 100 h of visible light irradiation were 86% for rhB and 80% for IC. Although the mineralization degree is similar in both organic dyes, the profile of the curves TOC vs. *t* is quite different. The temporal evolution of the TOC content in the experiment with rhB shows a quick reduction in the TOC value for the first 25 h of irradiation. After this time, the TOC content tends to have a semi-constant value. This behavior can be explained on the basis of the photocatalytic degradation mechanism of rhB proposed in this work. By taking into account that the photosensitization process is the predominant degradation mechanism, an important decrease in the TOC value takes place during the first hours, when the presence of rhB promotes its degradation by photosensitization. After 25 h of irradiation, the degradation of rhB intermediates can only take place by true photocatalysis, which is not a favorable process and then, the complete mineralization is difficult to be reached. On the other hand, for IC the temporal TOC value decreases following a zero order reaction. Due to the fact that the IC degradation occurs by simultaneous photosensitization and true photocatalysis processes, the bleaching of the solution does not affect considerably the mineralization process.

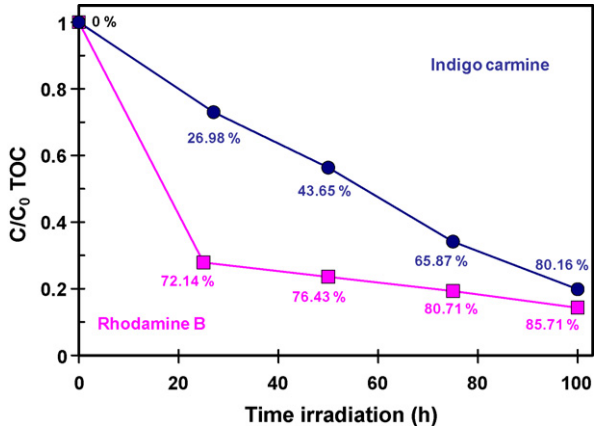

Fig. 9. Changes in the TOC during the mineralization of rhB and IC.

By taking into account the results obtained from the rhB- and IC-TOC experiments and the relatively easy mineralization of both organic dyes, an efficient removal of them from industrial wastewater can be predicted. Likewise, the co-precipitation route has shown to be an easy, efficient, and inexpensive method to prepare γ-Bi_2MoO_6 photocatalysts with high activity in the degradation of organic dyes under visible light irradiation.

4. Conclusions

The γ-Bi_2MoO_6 oxide was successfully synthesized by the co-precipitation method at 450 °C. This synthesis route provides a well crystallized material, formed by particles with heterogeneous shapes whose sizes are larger than 200 nm. The molybdate acted as a photocatalyst in the photocatalytic degradation of rhodamine B and indigo carmine under visible light irradiation. On the other hand, a negligible photocatalytic activity of γ-Bi_2MoO_6 was observed in the degradation of methyl orange due to the presence of the azo group. The analysis of total organic content of the samples irradiated at different times showed that the mineralization of rhodamine B and indigo carmine by a γ-Bi_2MoO_6 photocatalyst is feasible. Throughout the experiments with vis- and UV-irradiation, it was possible to conclude that the degradation of rhB by γ-Bi_2MoO_6 seems to occur predominantly through the photosensitization of the organic dye by the action of visible light irradiation, whereas the degradation of IC simultaneously happens by photosensitization and true photocatalysis processes.

Acknowledgements

We wish to thank to the Universidad Autónoma de Nuevo León (UANL) for its invaluable support through the projects PAICYT 2009 and to CONACYT for supports the project 81546. We also thank to Departamento de Ecomateriales y Energía of Facultad de Ingeniería Civil (UANL) for its assistance on the materials characterization.

References

[1] M.A. Rauf, S. Salman Ashraf, Chem. Eng. J. 151 (2009) 10.
[2] A. Kudo, Y. Miseki, Chem. Soc. Rev. 38 (2009) 253.
[3] S. Yang, L. Gao, J. Am. Ceram. Soc. 87 (2004) 1803.
[4] Z.G. Zou, J.H. Ye, K. Sayama, H. Arakawa, Nature 414 (2001) 625.
[5] J.W. Tang, Z.G. Zou, J.H. Ye, Chem. Mater. 16 (2004) 1644.

[6] Z. Zou, J. Ye, K. Sayama, H. Arakawa, Chem. Phys. Lett. 333 (2001) 57.
[7] A. Kudo, K. Omori, H. Kato, J. Am. Chem. Soc. 121 (1999) 11459.
[8] Y. Shimodaira, H. Kato, H. Kobayashi, A. Kudo, J. Phys. Chem. B 110 (2006) 17790.
[9] J. Yu, A. Kudo, Chem. Lett. 34 (2005) 1528.
[10] H. Li, C. Liu, K. Li, H. Wang, J. Mater. Sci. 43 (2008) 7026.
[11] H. Li, K. Li, H. Wang, Mater. Chem. Phys. 116 (2009) 134.
[12] X. Zhao, T. Xu, W. Yao, Y. Zhu, Appl. Surf. Sci. 255 (2009) 8036.
[13] A. Martínez-de la Cruz, S. Obregón Alfaro, E. López Cuéllar, U. Ortiz Méndez, Catal. Today 129 (2007) 194.
[14] H. Xie, D. Shen, X. Wang, G. Shen, Mater. Chem. Phys. 110 (2008) 332.
[15] X. Zhao, J. Qu, H. Liu, C. Hu, Environ. Sci. Technol. 41 (2007) 6802.
[16] Y. Man, R. Zong, Y. Zhu, Acta Phys.: Chim. Sin. 23 (2007) 1671.
[17] X. Zhao, J. Qu, H. Liu, Z. Qiang, R. Liu, C. Hu, Appl. Catal. B: Environ. 91 (2009) 539.
[18] J. Bi, L. Wu, J. Li, Z. Li, X. Wang, X. Fu, Acta Mater. 55 (2007) 4699.
[19] L. Zhou, W. Wang, L. Zhang, J. Mol. Catal. A: Chem. 268 (2007) 195.
[20] L. Xie, J. Ma, G. Xu, Mater. Chem. Phys. 110 (2008) 197.
[21] C. Belver, C. Adan, M. Fernández-García, Catal. Today 143 (2009) 274.
[22] A. Martínez-de la Cruz, S. Obregón Alfaro, Leticia M. Torres-Martínez, I. Juarez Ramirez, J. Ceram. Process. Res. 9 (5) (2008) 490.
[23] http://www.hach.com, Patent pending.
[24] L.M. Reilly, G. Sankar, C.R.A. Catlow, J. Solid State Chem. 148 (1999) 178.
[25] A.O. Remya Sudhakar, S. Mathew, Thermochim. Acta 451 (2006) 5.
[26] R. Gunawan, D. Zhang, J. Hazard. Mater. 165 (2009) 751.
[27] L. Xie, J. Ma, Z. Zhao, H. Tian, J. Zhou, Y. Wang, J. Tao, X. Zhu, Colloids Surf. A: Physycochem. Eng. Aspects 280 (2006) 232.
[28] J.B. Condon, Surface Area and Porosity Determinations by Physisorption, Elsevier, Amsterdam, 2006, ISBN 0-444-51964-5.
[29] J. Jung, H. Kim, A. Choi, Y. Chung, T. Kim, S. Lee, S. Oh, I. Song, Catal. Commun. 8 (2007) 625.
[30] B. Ohtani, Chem. Lett. 37 (2008) 217.
[31] A. Martínez-de la Cruz, U.M. García Pérez, Mater. Res. Bull. 45 (2010) 135.
[32] M. Stylidi, D.I. Kondarides, X.E. Verykios, Appl. Catal. B: Environ. 40 (2003) 271.